Title

A model exploring whether the coupled effects of plant water supply and demand affect the interpretation of water potentials and irrigation management

Journal

Agricultural Water Management, 192(C)

ISSN

0378-3774

Authors

Spinelli, Gerardo M
Shackel, Ken A
Gilbert, Matthew E

Publication Date

2017-10-01

DOI

10.1016/j.agwat.2017.07.019

Peer reviewed

Title. A model exploring whether the coupled effects of plant water supply and demand affect the interpretation of water potentials and irrigation management

Authors. **Gerardo M. Spinelli*, Ken A. Shackel, and Matthew E. Gilbert**

Affiliation. University of California, Davis, Dept. of Plant Sciences. One Shields Ave, Davis, CA 95616-8683, USA.

Corresponding author. Tel.: (530) 304 3738. *E-mail address*: gerardo.spinelli@gmail.com (G. Spinelli).

Abstract

Water potential is a useful predictive tool in irrigation scheduling as it, or a component, is associated with physiological responses to water deficit. Increasing atmospheric *demand* for water increases transpiration and decreases water potential for the same stomatal conductance. However, based on *supply* by the soil-plant-atmosphere-continuum, decreasing soil water potential should decrease stomatal conductance and thus transpiration but also decrease water potential. Such contradictory behavior of supply and demand responses, may limit the value of water potential as an indicator of plant water status. This work studied the relationship between plant water potential and transpiration affected by supply (soil moisture) and atmospheric evaporative demand, and has implications for interpretation of water potentials and irrigation management. Results were that plant water potential has a narrow range of sensitivity to variation in supply and demand in hydrated soils, but greatly varying sensitivity in dry soils, limiting interpretation under dry conditions. Loss of soil conductance in dry, coarse soil types affects the trajectory of plant water potential response to supply and demand. Sapflow measurements on almonds indicated that variation in reference evapotranspiration and/or soil moisture deficit led to similar variation in stem water potentials to that predicted by the model. The model indicates hypotheses that with further testing may have important repercussions on the measurement of plant water use and irrigation scheduling.

Keywords: sapflow, almond, *Prunus dulcis*, crop coefficient, water potential

Introduction

The responses of plants to water stress modulate physiological processes such as carbon assimilation, growth, reproductive success and water uptake (Hsiao, 1973). Thus, our understanding of water stress has

important implications for both physiological studies and practical applications such as irrigation scheduling.

Water potential (Ψ) is considered as particularly informative as it is related to many plant processes: it integrates the hydrostatic, gravitational, matric and osmotic effects on water availability. However, some authors have criticized the focus on Ψ, suggesting that relative water content or components of Ψ may be better indicators of physiological responses (Passioura, 1988; Sinclair and Ludlow, 1985). As relative water content measurements are prone to error (Arndt et al., 2015; Boyer et al., 2008), plant water potential has remained as a standard indicator of physiological and irrigation status. Leaf to leaf variability in water potential occurs due to differences in orientation and boundary layer conductance, and therefore stem water potential (Ψ_{stem}) can be used as a more averaged and stable indicator of plant water stress (Choné et al., 2001; Marsal et al., 2005; McCutchan and Shackel, 1992; Naor et al., 1995). Stem water potential, measured using light, pump-up pressure chambers, is being used to schedule irrigation in fruit and nut tree horticulture in California, in particular by the large almond industry (Goldhamer and Fereres, 2001; Shackel, 2011)

However, Ψ as a stress indicator relates to the fact that responses to water stress such as stomatal closure, senescence etc., are regulatory mechanisms that control transpiration (T). Thus, a stress-related decrease in T may totally or partially maintain Ψ_{leaf} (or Ψ_{stem}) in a physiological range (Jones, 1983; Jones, 1990). The degree to which this homeostasis of Ψ occurs is thought to be species and variety-dependent leading some authors to define isohydric (with a stable Ψ_{leaf} and strong stomatal control) and anisohydric (variable Ψ_{leaf} with weak stomatal control) behaviors in response to variation in evaporative demand (Klein, 2014; Schultz, 2003; Tardieu and Simonneau, 1998). Although species may show behaviors that fall on the continuum between aniso- and isohydry, for many species water potentials can be used as a proxy for water status, while stomata also exert considerable control over water status (Tardieu and Simonneau, 1998). In the case of almond, stomatal conductance is consistently linearly related with stem water potential (Egea et al., 2011; Spinelli et al., 2016). . For such species, the relationship of Ψ to T is the result of two opposite behaviors: first, a decrease in T is expected when Ψ decreases (more negative) due to stomatal closure under limited water supply; second, a drop in Ψ is expected as T increases due to increased demand. These two

behaviors are the basis of a heuristic model developed here to test the conflicting influence of coupled supply and demand factors on transpiration and water potential. The impact of the canopy energy balance is likely to be particularly important to incorporate in the model, as changes in stomatal conductance would be somewhat counteracted by the response of increasing temperature.

For the purposes of irrigation management, a proxy of the evapotranspiration of a crop (ET_c) can be calculated from multiplying the reference evapotranspiration for a grassy reference surface (ET_o) and the crop coefficient (K_c). The use of ET_o and ET_c assumes that the reference ET can be used to account for variation in evaporative demand when interpreting field transpiration data (Espadafor et al., 2013; Johnson et al., 2005; Williams et al., 2012). Similarly dividing an observed T by ET_o should detrend the T for variation in evaporative demand. However, ET_o is specifically for a grassy reference surface, not trees, and does not account for the feedbacks of Ψ on T and effects of soil moisture. Thus, the models developed below were also used to explore the effect of soil moisture and evaporative demand on the use of ET_o.

More broadly, this work is an attempt to capture the interdependence between transpiration and water potential in almonds, modeling the behavior of three interdependent variables (T, Ψ_{stem} and stomatal conductance) in a system of three equations/behaviors (Appendix). The three behaviors are: T decreases as stomata close, modeled with eqn. 1; Ψ decreases with T increases, modeled with eqn. 2; stomata close with decreasing Ψ_{stem}, based on an empirical relationship observed in almond (Spinelli, 2015). The model was run varying Ψ_{soil} and environmental variables affecting the evaporative demand of the atmosphere in order to mimic the natural conditions experienced by plants in the field. A validation of the model was attempted using sapflow velocity to estimate transpirational flow and measurements of Ψ_{stem}.

With the objective of investigating the validity of Ψ_{stem} as a predictor of T for almonds, this study explores the following questions through modelling and sap flow data:

1) What is the relationship of T with Ψ during supply (soil) and demand (atmosphere) limitations? How does changing soil conductivity over a soil dry-down affect this relationship?
2) Does stomatal conductance variation result in proportional variation in transpiration with soil drydown?

3) Do the interrelated variables affect the usefulness of grassy reference surface ET_o in irrigation management for tree crops?

Model development: A hydraulic model of supply and demand influences on transpiration

The response of transpiration (T) to variation in Ψ due to changing atmospheric demand can be described using an energy balance approach that calculates transpiration as a function of atmospheric variables and stomatal conductance, under the assumption that stomatal conductance has a monotonic relationship with Ψ (in the leaf or any other part of the plant) (Fig. 1). Thus the demand side response of canopy T to water potential can be modelled based upon the Penman-Monteith equation (Monteith and Unsworth, 1990), based upon the assumption that a mature almond orchard soil evaporation is low (see Appendix for more details):

$$T \cong LE = \frac{\Delta\,(R_n - G) + \rho C_p\, g_a (e_{sat(Ta)} - e_a)}{\Delta + \gamma\left(1 + \frac{g_a}{g_{c(\Psi)}}\right)} \qquad \text{(eqn. 1)}$$

T is transpiration or latent energy removal by soil and within-leaf evaporation (E), Δ is the slope of the relationship between vapor pressure and air temperature, R_n is net radiation, ρ is air density, C_p is air heat capacity at constant pressure, g_a is aerodynamic conductance, $e_{s(Ta)}$ is the saturated vapor pressure at air temperature; e_a is air vapor pressure; L is the latent heat of vaporization, γ is the psychrometric constant and $g_{c(\Psi)}$ is canopy conductance that is dependent on plant Ψ and based upon stomatal conductance's of individual leaves. Note that this general formulae is effectively the same as the reference ET_o formula used elsewhere (Allen et al., 1998), but has a unit transformation and lacks the specific constants for a grassy reference surface. The predicted relationship between T and water potential for varying evaporative demand (ET_o) is a decreasing line, where greater evaporative demand results in higher T and more negative Ψ (Fig. 1a). But, variation in soil water deficit results in T decreasing with lower Ψ at constant ET_o (Fig. 1b). The

demand and supply responses (Fig. 1a and b) are contrasting, but meet where the soil water potential and ET_o are the same. The supply function does not reach higher stem water potentials than ~ -1MPa for a constant ET_o (600 W m^{-2}) as the plant has a finite hydraulic conductance resulting in a gradient from the soil to the stem (Fig. 1b). The demand function increases to the point that stomata close considerably due to negative leaf or stem water potentials, but for the high soil water potential modelled the closure happens at unreasonably high ET_o's (>800 W m^{-2}; not shown).

The response of T to limited supply of water in the soil is based on the soil-plant-atmosphere continuum (SPAC) and is represented by the hydraulic flux-gradient relationship (Van den Honert, 1948), applicable to any two points in the SPAC:

$$T = \frac{\Psi_a - \Psi_b}{R_{a\_b}} = \frac{\Psi_{soil} - \Psi_{stem}}{R_{soil\_stem}} \qquad \text{(eqn. 2)}$$

Ψ is water potential at the point indicated in the subscript and R is the hydraulic resistance between the two points in consideration. Assuming steady-state conditions and an in-series pathway, T is the same in all successive segments of the transport pathway.

However, it is well known that R in the bulk soil increases as decreasing Ψ_{soil} determines a loss of soil conductivity (Campbell and Norman, 1998; Sperry et al., 1998) and that R in the xylem increases as a result of embolisms occurring at low Ψ_{xylem} (Tyree and Sperry, 1989). However, the usual range of water potentials in moderately water stressed almonds is >-3MPa and almond is not vulnerable to loss of stem conductivity i.e. 50% of stem conductivity is lost at ~ -6MPa for almonds (Cochard et al., 2008). Thus, the plant resistance was modelled as a constant, but the soil conductivity was modelled based upon soil-type specific parameters (Appendix). Leaf hydraulic conductance can vary with water status (Hernandez-Santana et al., 2016), and this was considered in the Discussion. Changing soil conductance is a function of the soil water potential between the root and bulk soil, and thus the soil loses conductance when plant transpiration rates reach a maximum value; the model presented in the Appendix represents this key response, and is consistent with Sperry et al. (2002).

Materials and Methods

Model application

The model used for these calculations is described in the Introduction and Appendix. The full coupled atmospheric/soil model was applied to ranges of environmental variables that are typical of midday conditions for an almond orchard during summer months in central California: air temperature 20 to 35 ˚C, soil water potential -0.001 to -1.5 MPa, aerodynamic conductance 33.3 mm/s (resistance 30 s/m), air vapor pressure 1400 Pa, net radiation 700 W m^{-2}, ground heat flux was assumed to be 10% of net radiation during the day (CIMIS, 2015). Canopy conductance was used in eqn. 1 in place of stomatal conductance applying the Big Leaf model described in Monteith and Unsworth (1990). Canopy conductance was calculated as an average of stomatal conductance for shaded and sunlit leaves weighted by the contribution to LAI of each class of leaves, as proposed by Sinclair *et al.* (1976). An average LAI of 3.25 was obtained from Zarate-Valdez *et al.* (2012) for the same orchard.

The variable nature of soil hydraulic conductivity was included in the model as a function of soil water potential; the Campbell and Norman (1998) equation was used with the factors indicated for a sandy loam and clay matching the soil types at the two experimental sites, Belridge and Davis, respectively.

The model was run to predict the behavior of the relationship between transpiration and Ψ_{stem} varying soil water potential and varying the evaporative demand of the atmosphere estimated as ET_o (Allen et al., 1998). Because of the widespread use of a constant midseason crop coefficient (K_c) for almonds in irrigation scheduling, the supply and demand responses of the modelled almond crop coefficient (K_a; $K_a = ET_a/ET_o$; where 'a' represents almonds) were also investigated.

Experimental sites

Sapflow data for model validation were collected in two almond (*Prunus dulcis* D.A Webb) orchards, one at the Paramount Farming Company in Belridge, California, and one at the Students' Orchard at UC Davis. In Belridge, Nonpareil trees grafted on Nemaguard were planted in a sandy loam at 6.4 X 7.9 m spacing. In Davis, Nonpareil trees were planted in a clay loam. Environmental variables and FAO 56 (Allen et al., 1998) grass reference evapotranspiration (ET_o) were obtained by the nearby CIMIS stations (Belridge station #146 and Davis #4). An attempt was made to calculate a more appropriate reference evapotranspiration for almond at midday (almond ET_o). The Penman-Monteith equation was used (eqn. 1) with the environmental variables obtained from CIMIS for the period 12 PM to 3 PM. A constant unstressed canopy resistance reference value of 75 s/m was used, obtained experimentally (Spinelli, 2015); aerodynamic resistance (r_a) was estimated from wind speed (u) using the empirical function $r_a = 30/u$ obtained from data reported in Spinelli (2015).

Sapflow and irrigation

Relative transpirational flow was estimated measuring sapflow velocity at both sites in almond trees during the summer of 2013. Sapflow velocity was measured with SFM1 Sap flow Meters (ICT International, Armidale, Australia) at a measurement depth of 12.5 and 27.5 mm from the bark. The highest flow rates occur at 20 to 30 mm depth in almond (M.E. Gilbert and H.K. Vice, pers. obs.). Data obtained from the probes at 12.5mm were discarded because there was no clear daily pattern and the rest of the data was screened for data quality. Measurement frequency was set at 30 min and the heat pulse was set at 40 J. The probes were installed at a distance of 6 mm from each other. Heat pulse velocity was calculated as proposed by Burgess *et al*. (2001) using the heat ratio method. Subsequently, the data was integrated over each day to obtain an estimate of relative daily transpiration for each tree. The xylem area contributing to sap flow for each probe is unknown, therefore the sapflow velocity data gives only relative information of the time pattern of each probe.

Three trees were chosen showing water status representative of the whole orchard i.e. a tree with average stem water potential, and trees with values similar to the highest and lowest stem water potentials measured atBelridge. The trees received conventional irrigation management of commercial almond orchards. In Davis, two trees with similar low initial water status were chosen and a high volume irrigation treatment (multiple microjet sprinklers were added per tree) was applied to one tree (#26), while the second tree received conventional irrigation (single microjet) (#22) maintaining the soil water deficit.

Ψ_{stem} and Ψ_{soil}

Ψ_{stem} was measured on fully expanded, lower canopy, shaded leaves, with pressure chambers (Soil Moisture Equipment and PMS Instruments). The leaves were enclosed in plastic and aluminum bags at least 20 minutes prior to excision and measurement. In some cases, two leaves per tree were measured and the values averaged. To estimate the degree of water stress, an unstressed baseline water potential based on air vapor pressure deficit was calculated for both sites following McCutchan and Shackel (1992).

At both sites, Ψ_{soil} was estimated with a soil moisture balance approach. The inputs were precipitation and the measured irrigation applied and the output was ET_a, calculated from ET_o from the nearby CIMIS station and assuming a constant crop coefficient of 1.15. Deep drainage and runoff were assumed to be negligible. Ψ_{soil} was estimated from soil moisture using water retention curves for the respective soils. A water retention curve for the soil at Belridge was obtained from Kandelous (pers. comm.) and at Davis a curve for a similar soil located 1.2 miles from the experimental site was obtained from Acevedo (1975). Ψ_{soil} was used to illustrate the periods where soil moisture was low – a heuristic – the values should not be interpreted as measured.

Results

Model predictions of the T to Ψ relationship for two soils

The modeled relationship between transpiration and Ψ_{stem} was curved for eight levels of Ψ_{soil} and four levels of ET_o (Fig. 2a). Starting from point A and following the solid curve to point B, the plot shows the expected relationship of transpiration and Ψ_{stem} during a hypothetical soil dry-down cycle at five time points (Fig. 2a). Each point has successively lower Ψ_{soil} -0.001 (point A), -0.1, -0.25, -0.5 and -0.75 MPa (point B) and all points on this curve have the same ET_o (418 W m^{-2}). This scenario shows that a positive correlation between transpiration and Ψ_{stem} is expected when the water potential in the soil is varied and ET_o is kept constant. In other words, when plant water potential decreases as a result of a drying soil, transpiration is expected to decrease. Furthermore, as the soil dries (i.e. following the curve from A to B), transpiration declines less dramatically in low ET_o conditions (curve with points A and B) than in high ET_o conditions (curve with point C).

In contrast, the four points from B to C represent four time points with a common Ψ_{soil} (-0.75 MPa) and increasing ET_o from 418 (point B), 485, 545, to 600 W m^{-2} (point C). In this case, a negative association is expected between transpiration and Ψ_{stem}. This is evidence that, when soil moisture is kept constant, a *decrease* in plant water potential caused by higher evaporative demand is associated with an *increase* in transpiration, opposite behavior to the soil water deficit response.

The slope of the T and Ψ_{stem} relationship (e.g. C to B), caused by variation in ET_o, changes with Ψ_{soil} for sandy loam soils, but little for clay (Fig. 2a and b). That is, the sensitivity of Ψ_{stem} to variation in ET_o is low for wet sandy loams (line with point A) and flatter (Ψ_{stem} is more sensitive) as the soil dries (i.e. at -1.5 MPa). For sandy loam soils the change in slope of the T and Ψ_{stem} response with variation in ET_o is caused by changing hydraulic conductivity in the soil as it dries. At high ET_o and low Ψ_{soil} the loss of water transit pathways in large pore/grains of the sandy loam soil causes loss of conductivity (Fig. 2b). However, the

hydraulic conductivity of clay soils is effectively not limiting to plant water uptake in the range of soil water potentials usually expected (0 to -1.5 MPa). These results indicate that Ψ_{stem} has variable sensitivity as a predictor of T, whenvariation occurs in either supply (Ψ_{soil}) or demand (ET_o), particularly for coarser soils such as sands.

Stem water potential as a predictor of water stress is also differentially sensitive to Ψ_{soil} (Fig. 3), with a ~0.8 MPa change in Ψ_{stem} for a 1 MPa change in Ψ_{soil} in wet soils (points A and B in Fig. 3). In dry soils the sensitivity varied by almost two fold, with 1 MPa change in Ψ_{stem} for a 1 MPa change in Ψ_{soil} for sandy loam at high ET_o, and a 0.55 MPa change in Ψ_{stem} for a 1 MPa change in Ψ_{soil} for clay at low ET_o (Fig. 3, points C and D). Within a usual range of well-irrigated soil water potentials (0 to -0.5 MPa), the sensitivities varied by 10% across the range of ET_o and soil types. With constant Ψ_{soil} (-0.5 MPa) and a variable ET_o, there is a negative correlation between transpiration and canopy conductance, but a positive correlation when only Ψ_{soil} varies (Fig. 4). This means that a decrease in canopy or stomatal conductance is not associated with a decrease in transpiration when evaporative demand increases, but they are linked with soil is drying. Similar relationships are present for stomatal conductance of sun exposed leaves which makes up the majority of canopy conductance. In other words, if soil wetness is kept constant, as the evaporative demand of the atmosphere increases, plant transpiration *increases*, despite a reduction in stomatal conductance and Ψ_{stem}.

ET_o response to demand

The modelled almond crop coefficient ($K_a = ET_a/ET_o$) and Ψ_{stem} (Fig. 2c and d) are similar to the transpiration responses (Fig. 2a and b). K_a decreases when Ψ_{stem} decreases because of a reduction in Ψ_{soil}. However, for almonds K_a shows an increase associated with a decrease in Ψ_{stem} when the evaporative demand of the atmosphere is increased. The slope of the K_a to Ψ_{stem} relationship under varying ET_o is steeper at high Ψ_{soil} and it gets flatter as the soil dries out for the sandy loam (Fig. 2d). At Ψ_{soil} = -1.25 MPa the slope is flat and the relationship between K_a and Ψ_{stem} is independent of ET_o. In theory, if the crop coefficient

K_a really accounted for the evaporative demand of the atmosphere, the relationship between K_a and Ψ_{stem} should always be flat as ET_o is varied. However, the data from the model show that K_a is independent of ET_o only at the drier end of the soil for sandy loam, but not for clay. This behavior of K_a suggests that using a constant K_c value is not the appropriate method to account for environmental variability tree crop water use studies, since ET_a is not uniquely related to ET_o in a proportional manner.

Measured response to variation in demand (Belridge site)

At the Belridge experimental site there was little variation in reference (grass) ET_o (Fig. 5a,b). Stem water potential data show a clear reduction during the second half of July and during the second week of August with each tree showing different magnitudes of water stress. Trees 142 and 266 showed moderate stress (-1.4 MPa and -1.6 MPa respectively) and tree 274 showed mild stress (-1.1 MPa). The estimated Ψ_{soil} showed little variation, due to the frequent irrigation events (weekly). The sapflow velocity data should be interpreted in relative terms, since the xylem area contributing to sap flow is unknown. However, sapflow velocity from all trees show common patterns associated with ET_o. For instance, all trees show a decrease of sapflow on July 9th (A), when a drop in ET_o was recorded and an increase on July 14th and 15th that is associated with an increase in ET_o adjusted for almonds (B). In contrast, all trees show an increase in sapflow velocity during days 7/20th, 7/21st, 7/22nd and 7/23rd, that is associated with a drop in Ψ_{stem}, but it is not associated with grass ET_o (C). However, the same four days of high sapflow are associated with high almond ET_o (Penman-Monteith ET_o calculated using almond reference values for aerodynamic and canopy conductance's) and a drop in Ψ_{stem} during the stress cycle between 7/17th and 7/31st. Based on the model, the increase in almond ET_o (based upon higher aerodynamic resistances than the reference crop) is likely to be the cause of the drop in Ψ_{stem}, on 7/23, but the short cut-off in irrigation may also have a role, although the estimated Ψ_{soil} did not decrease. Almond ET_o also showed a similar rise during 7/25th, 7/26th, 7/27th and 7/28th, but only tree #266 shows a similar pattern in sapflow (D). Conversely, the decrease in Ψ_{stem} during the first two weeks of August, is not associated an increase in ET_o and may be associated with soil moisture

depletion following the cut-off in irrigation (E). During that period, sapflow velocity decreased in all trees, although with different magnitudes.

Measured response to supply variation (Davis site)

At Davis (Fig. 6a,b), the Ψ_{stem} of both trees showed intense stress (-2 MPa) at the beginning of the experiment. Tree #26 responded to the subsequent high irrigation treatment with an increased Ψ_{stem} starting from 9/6th. Tree #26 kept improving its water status for the whole experiment, until almost reaching baseline on 10/1st, while tree #22 remained at the same level of water stress for the whole experiment. Many features in the pattern of sapflow of both trees are associated with ET_o, for instance, the rise of September 6th, 7th, 8th and 9th (A) and September 17th, 18th and 19th (B). However, while the stressed tree #22 showed a gradual reduction in sapflow velocity, the irrigated tree #26 showed a decrease at the beginning of the experiment but then kept relatively constant values when the water status of the tree improved. Thus, relative to tree #22, tree #26 showed an increase in sapflow during the course of the experiment, presumably associated to the increased stomatal conductance caused by its improved water status. Both trees show a peak in Ψ_{stem} on 9/21st, in association with a low ET_o day (C). Tree #26 showed a larger increase in Ψ_{stem}, presumably caused by the irrigation of 9/20th. However, the estimated Ψ_{soil} for tree #26 showed first a first decrease at the beginning of the experiment and then a sharp increase until reaching field capacity values around September 15th and until the end of the experiment.

In Belridge, the daily cumulative sapflow velocity showed a negative correlation with Ψ_{stem} for all trees (Fig. 7; $R^2 = 0.55$, $P = 0.032$). Based on the model, such relationship is expected when the variation in Ψ_{stem} is determined by ET_o, as would occur in this well irrigated orchard. In Davis, the two trees showed a different behavior (Fig. 7). For the continually water stressed tree (#22) the relationship was non-significantly negative ($R^2 = 0.50$, $P = 0.079$), consistent with variation in ET_o causing sap flow velocity variation for this tree under constant soil water deficit. However, the rewatered tree #26 had a more flat relationship between sapflow velocity and Ψ_{stem} ($R^2 = 0.27$, $P = 0.38$), consistent with changing Ψ_{soil} causing

variation in sap flow. Both ET_o and Ψ_{soil} varied simultaneously for these data; predictions from a multiple regression analysis (dashed lines in Fig.7) illustrates that for a high ET_o of 529 W m^{-2} the slope of the sap flow to Ψ_{stem} relationship was steeper than for a lower ET_o, similar to the model predictions in Fig. 2.

Discussion

Plant water potential responds to water supply *and* demand

The usefulness of plant water potential as an indicator of soil water status, and irrigation timing, is determined by the sensitivity of plant water potential to soil water content and atmospheric demand. If plant water potential is similarly sensitive across a range of variation in soil water and atmospheric demand, then the atmospheric demand can be detrended using a consistent baseline and plant water potential can be broadly used to predict soil water status and trigger irrigation. While stem water potential was similarly sensitive to soil water potential and evaporative demand under a range of environments and soil types, sensitivities diverged considerably when soils were dry. These effects were variably interactive with both soil type and evaporative demand, and warrant further evaluation.

In a soil dry-down cycle (i.e. moving from point A to B in Fig. 2a), the model predicted that time points with high ET_o show a more rapid decline of transpiration as soil dries out than low ET_o time points. This is supported by data from experimental studies (Denmead and Shaw, 1962) and theoretically confirmed in models (Cowan, 1965). However, the model presented here differs from Cowan's in a number of features. Cowan's model did not account for the dependence of soil conductivity on Ψ_{soil}. Secondly, stomatal conductance was assumed by Cowan to maintain a high constant value at high Ψ_{leaf} and to decline linearly once Ψ_{leaf} reached a threshold value, unlike what is observed in almonds.

A curved relationship between T and Ψ_{stem} is expected based on the Penman-Monteith equation (eqn. 1), where the difference in slope across different ET_o's is due to the stronger stomatal control associated with a more negative Ψ_{stem} that results from a larger transpiration flow. The sapflow data demonstrated similar responses to those predicted by the model: 1) that variation in ET_o and Ψ_{soil} result in contrasting relationships between T (sapflow) and Ψ_{stem}, 2) that the sensitivity of the relationship of T to Ψ_{stem} changes with ET_o (Fig. 7). The prediction of a decreasing K_a and T with soil water deficit is similar to lysimeter experiment data where dry downs corresponded to lower transpiration and plant water potentials in peaches and grapes (Johnson et al., 2005; Williams et al., 2012).

Relationships between ET_o and Ψ_{stem} have been used to develop baselines, or reference well-watered Ψ_{stem} values, that account for the effects of evaporative demand on Ψ to aid irrigation management (McCutchan and Shackel, 1992; Ortuño et al., 2006). Such relationships are of great practical value. As a predictor of Ψ_{soil}, the model showed that stem water potential was similarly sensitive (0.91 to 0.76 MPa change in Ψ_{stem} for 1 MPa change in Ψ_{soil}) above a Ψ_{soil} of -0.5MPa for any range of ET_o or soil type (Fig. 2a,b and Fig. 3). Thus it seems reasonable to use Ψ_{stem} to predict irrigation scheduling on the basis of limiting Ψ_{soil} down to a Ψ_{soil} of -0.5MPa. Furthermore, baseline "well-watered" values for Ψ_{stem}, based upon ET_o or vapor pressure deficit should function well in accounting for the consistent effects of evaporative demand on Ψ_{stem}.

However, in more dry soils (< -0.5MPa) there was decreasing sensitivity of Ψ_{stem} to Ψ_{soil} for clay soils and divergence of sensitivities to variation in ET_o (Fig. 2a and 3). Sandy loam soils displayed the opposite behavior, increasing sensitivity and sudden divergence of sensitivities to variation in ET_o under very dry soils (Fig. 2b and 3). The latter behavior is due to the increasing resistance of water flow in dry soils for coarse sandy soils. Thus, baseline "well-watered" values for Ψ_{stem} will become more difficult to apply in dry soils where the effects would be non-linear, and would vary based upon soil type.

The use of stem water potential for scheduling irrigation is essentially a trigger, where divergence from a baseline value indicates the need for irrigation to maintain full soil hydration. Thus changing sensitivity of stem water potential to soil hydration will not greatly affect its use as a binary trigger for irrigation,

particularly as soil water potentials should rarely be lower than -1MPa in high productivity orchards. However, changing sensitivity of stem water potential would be important when scheduling irrigation in severe regulated deficit conditions, or when using plant water potentials in research.

When considering orchards grown on sandy or coarse soil types, researchers/growers should be aware of the potential for runaway loss of soil conductivity under conditions of considerable soil water deficit and/or high evaporative demand. This effect is analogous to the runaway cavitation in the xylem of trees (Tyree and Sperry, 1988); a very negative water potential in a xylem vessel leads to cavitation of that vessel, in turn the loss of the conductive capacity of the vessel results in a greater burden on the remaining vessels leading to more negative water potentials and more cavitation. Similarly, runaway loss of soil conductivity would occur when large water filled spaces between soil particles will be sucked dry and these high conductivity pathways to the root lost under conditions of negative soil water potentials and/or negative root water potentials caused by high evaporative demand. The loss of the conductive capacity of large pores would then result in more negative water potentials in the roots and soil adjacent to the roots and, in turn, result in loss of conductivity in smaller pores – and runaway conductivity loss. Thus, it is possible, in coarse soils, for a plant to effectively lose contact with the water in the soil around its roots. These effects are limited to soils that have large pore sizes, and would not occur in physiologically meaningful conditions for smaller particle loams and clays. Coarse organic soils would also have the potential for this effect under drought conditions (Jones and Tardieu, 1998). These 'runaway soil conductivity' effects are similar to those in Sperry *et al*. (1998) who predicted that soil can be the limiting segment of the soil-plant system at high flow rates (a maximum transpiration).

Runaway stem xylem cavitation is less likely in almonds, as the percentage of loss of xylem conductivity for almond trees reaches values close to 20% only at Ψ_{stem} of -5 MPa (Cochard et al., 2008). In the range of Ψ_{stem} commonly observed in the field (0 to -3 MPa) the percentage loss of conductivity is less than 1%. In this context, the avoidance of loss of stem xylem conductivity seems not to be the most important priority in the optimization of stomatal control in almond trees. Leaf conductance may limit water transport to a greater degree in almonds (Hernandez-Santana et al., 2016). However, the negative water

potentials needed to result large conductance loss and the larger effect of soil conductivity change led to limited influence of leaf conductance loss on the results (not shown).

In summary, both a decrease and an increase in transpiration can be theoretically expected as Ψ_{stem} decreases depending upon the variation in soil or atmospheric moisture. In reality both behaviors are always superimposed on each other. Thus, the model suggests that in general it may be problematic to predict T from Ψ_{stem} without knowledge of Ψ_{soil} and R_{soil}.

Utility of ET_o and a constant crop coefficient for irrigation management

A constant crop coefficient (K_c) and local grassy reference ET_o are routinely used for determining how much irrigation water to apply. However, the actual crop coefficient for almonds (K_a) may be variable with supply and demand, and if so, a constant crop coefficient would be biased. However, the modelling done here shows that K_a is not a constant and varies with ET_o, soil water and soil type (Fig. 2). If K_a served the purpose it is used for, the relationship of K_a to ET_o should be flat lines. However, only at Ψ_{soil} of -1.25 MPa for sandy loam, did K_a show a constant value irrespective of the level of ET_o. The limitations of K_a have been shown elsewhere (Annandale and Stockle, 1994), and thus it seems more appropriate to calculate a crop-specific unstressed reference ET rather than using grass ET_o to account for environmental variability. However, it is remarkable that in wetter soil conditions, and consequently at higher stomatal conductance, the model output shows that K_a increases strongly as ET_o rises. This result is likely to be determined by the fact that aerodynamic resistance for grass is usually higher than for a crop, particularly a tall crop like almond. Therefore, if the soil water potential is assumed constant, a higher ET_o day results in a more-than-proportionally higher ET_a and hence in a higher K_a. A higher ET_a day can be associated with a lower Ψ_{stem} (eqn. 2), such conditions could result in both a higher K_a and a lower Ψ_{stem}, resulting in the counterintuitive scenario where a lower Ψ_{stem} is associated with a higher K_a.

In general, the model results are corroborated by experimental observations at the Belridge site (Fig. 5, 7). Presumably, in those conditions, short-term fluctuations of high evaporative demand were associated

with lower Ψ_{stem} and more than proportionally higher ET_a and hence sapflow velocity. Thus, sapflow shows a negative correlation with Ψ_{stem}. On the other hand, in Davis, where a gradual water status recovery occurred over a long period of time, a more flat relationship of sapflow and Ψ_{stem} was observed (Fig. 7). In this case, Ψ_{stem} appears to be consistent with the output from the model where Ψ_{soil} is varied. In the Davis experiment, Ψ_{stem} may be mostly influenced by soil wetness, although the variability in ET_o observed in Davis is larger than what observed in Belridge.

In conclusion, the model presented in this work suggests that water potential, despite being a robust index of many physiological processes, appears to be a good predictor of Ψ_{soil} in well-watered conditions, but not with low soil water availability and highly variable atmospheric evaporative demand in almonds. Additionally, the model suggests that baselines for irrigation scheduling may need to be improved to incorporate the role of decreased conductivities in the soil-plant system at low soil and plant Ψ. Furthermore, the model shows that the use of a constant crop coefficient for almonds does not properly account for atmospheric evaporative demand, particularly in wet soil conditions, and suggests that the use of crop-specific unstressed reference ET appears to be a better solution. Finally, the experimental validation of the model presented in this study is limited and more research is needed to validate the model implications.

Acknowledgements

The generous support of the Paramount Farming Company for use of the Belridge orchard is gratefully acknowledged. This project was supported by the USDA National Institute of Food and Agriculture, Hatch project number #1001480 to M.E.G, and Almond Board of California grants to M.E.G. and K.S.

Conflict of Interest

The authors report no conflicts of interest.

References

Acevedo, H., 1975. The growth of maize (*Zea mais* L.) under under field conditions as affected by its water relations. UC Davis.

Allen, R., Pereira, L., Raes, D., Smith, M., 1998. Crop evapotranspiration. Guidelines for computing crop water requirements (Irrigation and drainage paper 56). Food and Agriculture Organization, Rome.

Annandale, J., Stockle, C., 1994. Fluctuation of crop evapotranspiration coefficients with weather: a sensitivity analysis. Irrigation Sci 15, 1-7.

Arndt, S.K., Irawan, A., Sanders, G.J., 2015. Apoplastic water fraction and rehydration techniques introduce significant errors in measurements of relative water content and osmotic potential in plant leaves. Physiol Plant, 355-368.

Boyer, J.S., James, R.A., Munns, R., Condon, T.A., Passioura, J.B., 2008. Osmotic adjustment leads to anomalously low estimates of relative water content in wheat and barley. Funct Plant Biol. 35, 1172-1182.

Burgess, S.S., Adams, M.A., Turner, N.C., Beverly, C.R., Ong, C.K., Khan, A.A., Bleby, T.M., 2001. An improved heat pulse method to measure low and reverse rates of sap flow in woody plants. Tree Physiol 21, 589-598.

Campbell, G., Norman, J., 1998. An introduction to environmental biophysics. Springer, New York.

Choné, X., Van Leeuwen, C., Dubourdieu, D., Gaudillère, J.P., 2001. Stem water potential is a sensitive indicator of grapevine water status. Annals Bot 87, 477-483.

CIMIS, 2015. California Irrigation Management Information System. California Department of Water Resources, Sacramento, CA.

Cochard, H., Barigah, S.T., Kleinhentz, M., Eshel, A., 2008. Is xylem cavitation resistance a relevant criterion for screening drought resistance among *Prunus* species? J Plant Physiol 165, 976-982.

Cowan, I., 1965. Transport of water in the soil-plant-atmosphere system. J Applied Ecol 2, 221-239.

Denmead, O., Shaw, R.H., 1962. Availability of soil water to plants as affected by soil moisture content and meteorological conditions. Agron J 54, 385-390.

Egea, G., Dodd, I.C., González-Real, M.M., Domingo, R., Baille, A., 2011. Partial rootzone drying improves almond tree leaf-level water use efficiency and afternoon water status compared with regulated deficit irrigation. Functional Plant Biology 38, 372-385.

Espadafor, M., Lorite, I., Orgaz, P., Testi, L., Fereres, E., 2013. Assesing Almond Orchard Water Use: Evaluation of Methods, VI International Symposium on Almonds and Pistachios 1028, pp. 341-345.

Goldhamer, D., Fereres, E., 2001. Simplified tree water status measurements can aid almond irrigation. Cal Agr 55, 32-37.

Hernandez-Santana, V., Rodriguez-Dominguez, C.M., Fernández, J.E., Diaz-Espejo, A., 2016. Role of leaf hydraulic conductance in the regulation of stomatal conductance in almond and olive in response to water stress. Tree Physiology 36, 725-735.

Hsiao, T.C., 1973. Plant responses to water stress. Annual Rev Plant Physiol 24, 519-570.

Johnson, R., Williams, L., Ayars, J., Trout, T., 2005. Weighing lysimeters aid study of water relations in tree and vine crops. Cal Agr 59, 133-136.
Jones, H., 1983. Estimation of an effective soil water potential at the root surface of transpiring plants. Plant, Cell & Environ 6, 671-674.
Jones, H., 1992. Plants and microclimates: a quantitative approach to environmental plant physiology Cambridge University Press, Cambridge.
Jones, H., Tardieu, F., 1998. Modelling water relations of horticultural crops: a review. Sci Hort 74, 21-46.
Jones, H.G., 1990. Physiological aspects of the control of water status in horticultural crops. HortScience 25, 19-26.
Klein, T., 2014. The variability of stomatal sensitivity to leaf water potential across tree species indicates a continuum between isohydric and anisohydric behaviours. Functional Ecology 28, 1313-1320.
Koumanov, K., Hopmans, J., Schwankl, L., Andreu, L., Tuli, A., 1997. Application efficiency of micro-sprinkler irrigation of almond trees. Agricultural Water Management 34, 247-263.
Marsal, J., Girona, J., Basile, B., Dejong, T., 2005. Heterogeneity in fruit distribution and stem water potential variations in peach trees under different irrigation conditions. J Hort Sci Biotech 80, 82-86.
McCutchan, H., Shackel, K., 1992. Stem-water potential as a sensitive indicator of water stress in prune trees (*Prunus domestica* L. cv. French). J Am Soc Hort Sci 117, 607-611.
Monteith, J., Unsworth, M., 1990. Principles in environmental physics. Edward Arnold, London.
Naor, A., Klein, I., Doron, I., 1995. Stem water potential and apple size. J Amer Soc Hort Sci 120, 577-582.
Ortuño, M., García-Orellana, Y., Conejero, W., Ruiz-Sánchez, M., Mounzer, O., Alarcón, J., Torrecillas, A., 2006. Relationships between climatic variables and sap flow, stem water potential and maximum daily trunk shrinkage in lemon trees. Plant Soil 279, 229-242.
Passioura, J., 1988. Response to Dr PJ Kramer's article,'Changing concepts regarding plant water relations'. Volume 11, Number 7, pp. 565–568. Plant, Cell & Environ 11, 569-571.
Ritchie, J.T., 1972. Model for predicting evaporation from a row crop with incomplete cover. Water resources research 8, 1204-1213.
Schultz, H.R., 2003. Differences in hydraulic architecture account for near-isohydric and anisohydric behaviour of two field-grown *Vitis vinifera* L. cultivars during drought. Plant, Cell & Environ 26, 1393-1405.
Shackel, K., 2011. A plant-based approach to deficit irrigation in trees and vines. HortScience 46, 173-177.
Sinclair, T., Ludlow, M., 1985. Who taught plants thermodynamics? The unfulfilled potential of plant water potential. Funct Plant Biol 12, 213-217.
Sinclair, T., Murphy, C., Knoerr, K., 1976. Development and evaluation of simplified models for simulating canopy photosynthesis and transpiration. J Appl Ecol 13, 813-829.
Sperry, J.S., Adler, F., Campbell, G., Comstock, J., 1998. Limitation of plant water use by rhizosphere and xylem conductance: results from a model. Plant, Cell & Environ 21, 347-359.
Sperry, J.S., Hacke, U., Oren, R., Comstock, J., 2002. Water deficits and hydraulic limits to leaf water supply. Plant, Cell & Environment 25, 251-263.
Spinelli, G., 2015. Water stress and water use of almonds (*Prunus dulcis*) in California: Linking plant water status and canopy transpiration UC Davis available at www.ProQuest.com.
Spinelli, G.M., Snyder, R.L., Sanden, B.L., Shackel, K.A., 2016. Water stress causes stomatal closure but does not reduce canopy evapotranspiration in almond. Agricultural Water Management 168, 11-22.
Tardieu, F., Simonneau, T., 1998. Variability among species of stomatal control under fluctuating soil water status and evaporative demand: modelling isohydric and anisohydric behaviours. J Exp Bot 49, 419-432.
Tetens, O., 1930. Uber einige meteorologische Begriffe. Z. Geo- Phys. 6, 297-309.
Tyree, M.T., Sperry, J.S., 1988. Do woody plants operate near the point of catastrophic xylem dysfunction caused by dynamic water stress? Answers from a model. Plant Physiol 88, 574-580.

Tyree, M.T., Sperry, J.S., 1989. Vulnerability of xylem to cavitation and embolism. Annual Rev Plant Biol 40, 19-36.
Van den Honert, T., 1948. Water transport in plants as a catenary process. Discuss Faraday Soc 3, 146-153.
Williams, L., Baeza, P., Vaughn, P., 2012. Midday measurements of leaf water potential and stomatal conductance are highly correlated with daily water use of Thompson Seedless grapevines. Irrigation Sci 30, 201-212.
Zarate-Valdez, J.L., Whiting, M.L., Lampinen, B.D., Metcalf, S., Ustin, S.L., Brown, P.H., 2012. Prediction of leaf area index in almonds by vegetation indexes. Comp Elec Agri 85, 24-32.

Appendix: Full set of equations to describe the coupled soil and atmosphere model

The empirical linear relationship between stomatal conductance and stem water potential for sunlit (*_sun*) and shaded (*_sh*) leaves (Spinelli, 2015) used in the model is:

$$g_{sun} = 0.473 + 0.173 * \Psi_{stem}$$

$$g_{shade} = 0.3161 + 0.12 * \Psi_{stem}$$

Where Ψ_{stem} is in MPa units, g_{sun} and g_{shade} units of mol m^{-2} s^{-1} and are limited by a minimum of 0.02 mol m^{-2} s^{-1}. These equations are based upon measurements on almond trees at a range of sites and conditions (R^2 = 0.74 for sunlit leaves and R^2=0.43 for shaded leaves) and is reported in Spinelli (2015).

To obtain canopy conductance (g_c), sunlit and shaded leaves conductance's were scaled-up weighting the contribution to LAI (unitless) of each category (Sinclair et al., 1976):

$$g_c = LAI_{sun}\, g_{sun} + LAI_{shade}\, g_{shade}$$

Canopy conductance was converted from units of mol m^2 s^{-1} to m s^{-1} by dividing by the molar volume of air V_m = 40 mol m^{-3} (Jones, 1992).

The fraction of LAI of sunlit leaves was obtained assuming a horizontal distribution (Jones, 1992):

$$LAI_{sun} = 1 - e^{-LAI}$$

The fraction of shaded leaves was calculated by difference. A mean value of LAI = 3.25 was obtained from Zarate-Valdez et al. (2012).

The relationship between transpiration (LE, units W m^{-2}) and canopy conductance was obtained from the Big Leaf model (Monteith and Unsworth, 1990):

$$T = LE = \frac{\Delta\,(Rn - G) + \rho C_p\, g_a (e_{sat(Ta)} - e_a)}{\Delta + \gamma\left(1 + \frac{g_a}{g_{c(\Psi_{stem})}}\right)}$$

564

565 E is transpiration (Kg m^{-2} s^{-1}), Δ is the slope of the relationship between vapor pressure and temperature at
566 air temperature (Pa K^{-1}), R_n is net radiation (W m^{-2}), ρ is air density (Kg m^3), C_p is air heat capacity at
567 constant pressure (1204 J K^{-1} Kg^{-1}), g_a is aerodynamic conductance (m s^{-1}), $e_{s(Ta)}$ is the saturated vapor
568 pressure at air temperature (Pa); e_a is air vapor pressure (Pa); L is the latent heat of vaporization ($2.26x10^6$
569 J Kg^{-1}), γ is the psychrometric constant (67 Pa K^{-1}) and $g_{c(\Psi stem)}$ is canopy conductance (m s^{-1}) as a function
570 of plant Ψ. The model is based upon the calculation that soil evaporation is a minor component of total ET
571 in a high LAI almond orchard. For five year old almonds, microjet sprinklers operating every 2 or 3 days
572 resulted in soil evaporation of 0.5 to 1 mm day^{-1} (Koumanov et al., 1997), which was approximately 8.5 to
573 17% of total ET. In the mature orchards studied here having greater canopy cover of the soil, and with
574 longer periods between irrigation, it is expected that soil evaporation would be a smaller percentage of the
575 total orchard ET. Specifically, the energy-limited evaporation rate would result in higher evaporation for a
576 limited period after soil wetting, and then the water movement-limited phase of soil evaporation would
577 occur for most of the period between the weekly irrigation events (Ritchie, 1972) resulting in relatively low
578 contribution of soil evaporation to ET. In these circumstances, it seems valid to assume that transpiration
579 is approximated by ET.

580 The slope of the vapor pressure and temperature relationship (Δ, units Pa K^{-1}) was obtained as:

581

582 $$\Delta = \frac{4.098\ 10^6 \left(0.6108 \exp(\frac{17.27\ T_{air°C}}{T_{air°C} + 237.3})\right)}{(T_{air°C} + 237.3)^2}$$

583

584 Saturated air vapor pressure as a function of air temperature ($e_{sat(Ta)}$, units kPa) was obtained from Tetens
585 (1930):

586

587

588 $$e_{sat(Ta)} = 0.6108\ * \exp\left(\frac{17.27\ T_{air°C}}{T_{air°C} + 237.3}\right)$$

589

The relationship between stem water potential (Ψ_{stem}, units MPa) and transpiration (LE, units W m^{-2}) was obtained rearranging the classic equation from van den Honert (1948):

$$\Psi_{stem} = \Psi_{soil} - (LE\ R_{tot})$$

where R_{tot} (W MPa^{-1} m^{-2}) is the total resistance of the soil-plant system from the bulk soil to the stem. This resistance was obtained experimentally forcing Ψ_{stem} = 0 MPa at LE = 0 W m^2 and Ψ_{stem} = -1.2 MPa at LE = 700 W m^2. The first point is derived from theoretical considerations, while the second reflects the typical values observed in summer at midday in California for almonds in a well irrigated soil.

The soil-plant water transport system was modeled as a two-segment pathway with two resistances in series, R_p, resistance in the plant and R_{soil}, resistance in the soil, both with units of W MPa^{-1} m^{-2}:

$$R_{tot} = R_p + R_{soil}$$

Bulk soil saturated hydraulic conductivity was converted to units of W MPa^{-1} m^{-2} using the latent heat of vaporization (L=2.26 10^6 J Kg^{-1}) and water density (ρ_w = 10^3 Kg m^{-3}). The effects of soil water potential in limiting soil conductivity was modeled using the equation given in Campbell and Norman (1998):

$$K_{(\Psi soil)} = K_s \left(\frac{\Psi_e}{\Psi_{soil}}\right)^{2+\frac{3}{b}}$$

A value of -0.0091 or -0.0598 MPa was used for Ψ_e (air entry value of the soil for sandy loam and clay, respectively) and 3.31 or 14.95 was used for the parameter b, and 53.2 or 1.69 for K_s, respectively (Campbell and Norman, 1998). To obtain bulk soil resistance (R_{soil}) the inverse of $K_{\Psi soil}$ was taken. The $K_{(\Psi soil)}$ was scaled to the soil volume root geometry using the conversion of Sperry et al. (1998): with root length density, 10000 m of root m^{-3}; soil depth, 0.5m; and root radius, 1mm. The Ψ_{soil} used for $K_{\Psi soil}$ was taken as the geometric mean of Ψ_{root} and bulk Ψ_{soil}. Once soil resistance for a wet soil was obtained from

614 the equations above, plant resistance in absence of cavitation (R_p, units MPa m^2 W^{-1}) was obtained from

615 the difference:

616

$$R_p = R_{tot} - R_{soil} \quad (617)$$

618 Plant resistance was kept constant.

Table 1 Variables and units used in the model

Symbol	Quantity	Unit
b	Exponent of the soil moisture release equation	Unitless
C_p	Air heat capacity at constant pressure	1204 J K^{-1} Kg^{-1}
e	base of the natural logarithm	2.71828 Unitless
e_a	Air vapor pressure	Pa
$e_{sat(Tair)}$	Saturated vapor pressure at air temperature	Pa
g_a	aerodynamic conductance	m s^{-1}
g_c	canopy conductance	m s^{-1}
g_s	stomatal conductance	m s^{-1}
g_{sun}	stomatal conductance of sunlit leaves	mol m^2 s
g_{shade}	stomatal conductance of shaded leaves	mol m^2 s
G	Ground heat flux	W m^{-2}
K_a	Crop coefficient, ratio of actual to reference ET	Unitless
K_s	Soil saturated conductivity	W MPa^{-1} m^{-2}
$K_{(\Psi soil)}$	Soil conductivity as a function of Ψ_{soil}	W MPa^{-1} m^{-2}
LAI	Leaf area index	Unitless
LE	Transpiration or Latent heat flux	W m^{-2}
R_n	Net radiation	W m^{-2}
R_p	plant hydraulic resistance	W MPa^{-1} m^{-2}
R_{soil}	soil hydraulic resistance	W MPa^{-1} m^{-2}
R_{tot}	hydraulic resistance of the soil-plant system	W MPa^{-1} m^{-2}
T_a	Air temperature	K
$T_{air^\circ C}$	Air temperature in Celsius	˚C
γ	Psychrometric constant	67 Pa K^{-1}
Δ	Slope of the vapor pressure and temperature relationship	Pa K^{-1}
ρ	Air density	Kg m^{-3}
Ψ_e	Soil air entry value	MPa
Ψ_{soil}	Soil water potential	MPa
Ψ_{stem}	Midday stem water potential	MPa

624

625

626

627

Figure legends

Fig. 1 A coupled model of demand and supply effects on the response of transpiration (T) to plant water potential (Ψ_{stem}). Demand effects assume a monotonic relationship between stomatal conductance in the sun and shade (g_{sun} and g_{shade}) and Ψ_{stem} (1), and a scaling relationship to calculate canopy conductance (2). Based upon the Penman-Monteith model, demand side variation in atmospheric conditions result in a negative response of T to Ψ_{stem} (panel a). The supply effects can be based upon cavitation effects on stem resistance (3; R_{stem}; these effects were not used in this model) and effects on soil resistance (4) due to variation in water potential between the bulk soil (Ψ_{soil}) and root surface ($\Psi_{root\ surface}$). Based upon the SPAC hydraulic model the supply effects result in a curved positive relationship (panel b). The predicted relationships are for clay, where little effect of soil conductance is expected. The full model is detailed in the Appendix.

Fig. 2 Response of transpiration (panel a and b) or modelled crop coefficient ($K_a = T/ET_o$ of a grassy reference; panel c and d) under conditions of varying Ψ_{soil} and ET_o for two soil types (clay: panels a and c; sandy loam: panels b and d). These points are the predictions of the model encapsulated in eqn. 1 and 2, and run for four levels of ET_o (varying air temperature) and eight levels of soil water potential.

Fig. 3 Change in sensitivity of Ψ_{stem} ($\Delta\Psi_{stem}/\Delta\Psi_{soil}$) in response to variation in Ψ_{soil} and ET_o for two soil types. Data are the same as in Fig. 2.

Fig. 4 A positive relationship between transpiration and stomatal or canopy conductance under varying Ψ_{soil} and a negative relationship under varying ET_o for a constant Ψ_{soil}. These data are the same as Fig. 2, restricted to the highest ET_o (and Ψ_{soil} varied) or a Ψ_{soil} of -0.5 MPa (and ET_o varied). The contrasting

behavior of supply (circles) and demand (triangles) responses of transpiration to canopy conductance is evident at higher conductance.

Fig. 5 Temporal pattern of daily cumulative sapflow velocity and stem water potential (Ψ_{stem}) of three trees at the Belridge site (a) and temporal pattern of grass reference evapotranspiration (ET_o, from FAO 56, Allen *et al.,* 1998) and almond reference evapotranspiration for midday conditions in Belridge (b). Irrigation water applied and the baseline for stem water potential are also indicated. The soil water potential (Ψ_{soil}) was estimated to illustrate when soil moisture was limiting.

Fig. 6 Temporal pattern of daily cumulative sapflow velocity and stem water potential (Ψ_{stem}) of three trees at the Davis site (a) and temporal pattern of grass reference evapotranspiration (ET_o, from FAO 56, Allen *et al.,* 1998) and almond reference evapotranspiration for midday conditions in Davis (b). Irrigation water applied and the baseline for stem water potential are also indicated. The soil water potential (Ψ_{soil}) was estimated to illustrate when soil moisture was limiting.

Fig. 7 Sap flow velocity relationship with stem water potential for tree 26 in Davis (circles) undergoing rehydration from water deficit, tree 22 in Davis under soil water deficit and varying ET_o (Fig. 6), and three trees in Belridge (squares) with uniform irrigation and low variation in ET_o (Fig. 5). Dashed lines are fitted relationships between sap flow and water potentials for two constant ET_o values (averages for the two sites) derived from a multiple regression analysis: sap flow = $-879 - 317*\Psi_{stem} + 3.45*ET_o + 0.98*ET_o*\Psi_{stem}$ with $P < 0.001$, $P < 0.001$ and $P = 0.029$ for each factor, respectively.

Figures:

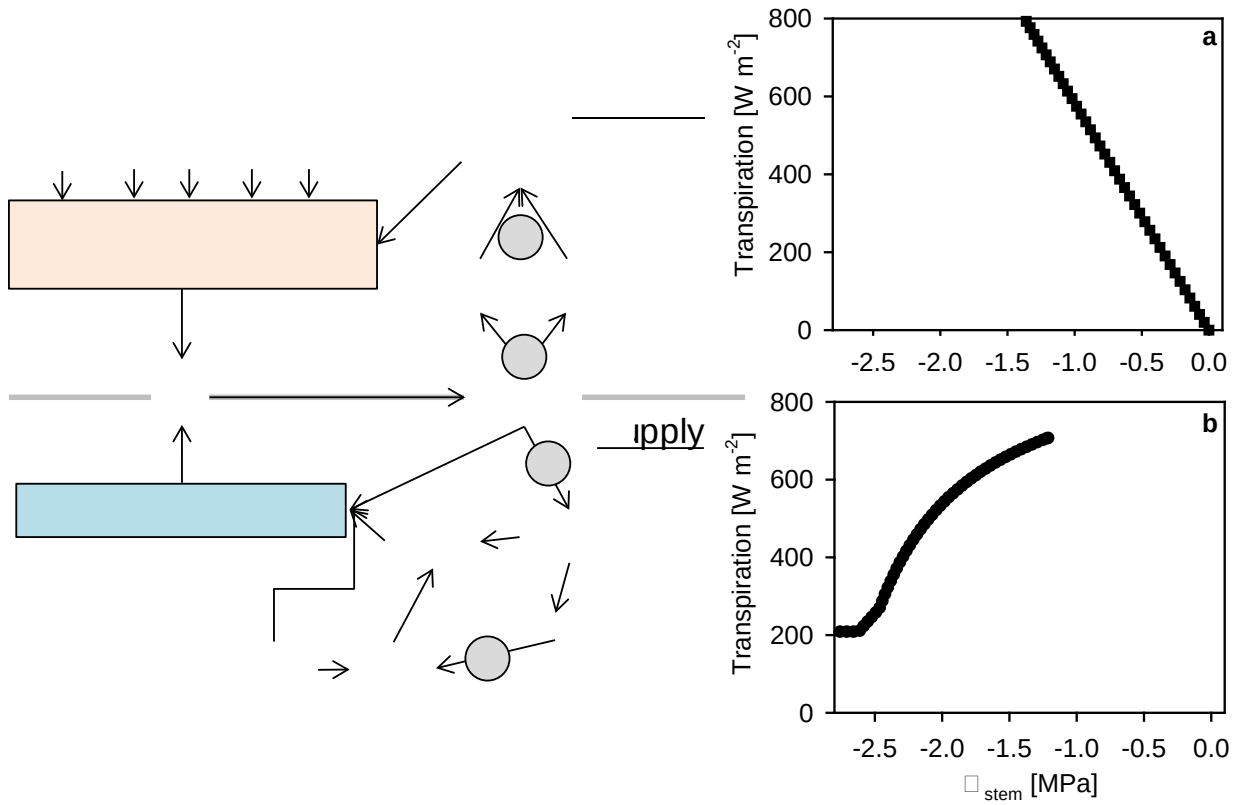

Fig. 1 A coupled model of demand and supply effects on the response of transpiration (T) to plant water potential (Ψ_{stem}). Demand effects assume a monotonic relationship between stomatal conductance in the sun and shade (g_{sun} and g_{shade}) and Ψ_{stem} (1), and a scaling relationship to calculate canopy conductance (2). Based upon the Penman-Monteith model, demand side variation in atmospheric conditions result in a negative response of T to Ψ_{stem} (panel a). The supply effects can be based upon cavitation effects on stem resistance (3; R_{stem}; these effects were not used in this model) and effects on soil resistance (4) due to variation in water potential between the bulk soil (Ψ_{soil}) and root surface ($\Psi_{root\ surface}$). Based upon the SPAC hydraulic model the supply effects result in a curved positive relationship (panel b). The predicted relationships are for clay, where little effect of soil conductance is expected. The full model is detailed in the Appendix.

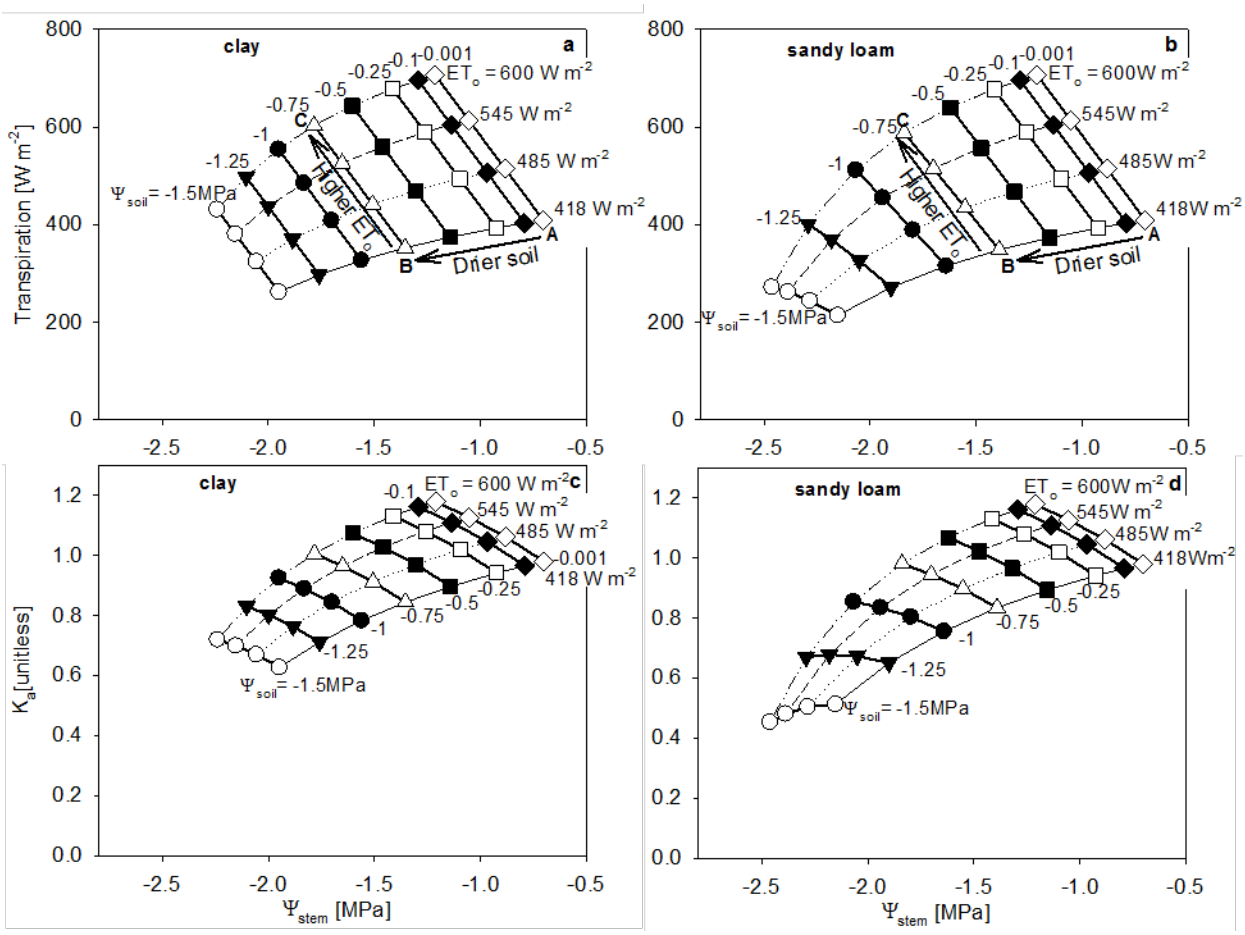

Fig. 2 Response of transpiration (panel a and b) or modelled crop coefficient (K_a = T/ET_o of a grassy reference; panel c and d) under conditions of varying Ψ_{soil} and ET_o for two soil types (clay: panels a and c; sandy loam: panels b and d). These points are the predictions of the model encapsulated in eqn. 1 and 2, and run for four levels of ET_o (varying air temperature) and eight levels of soil water potential.

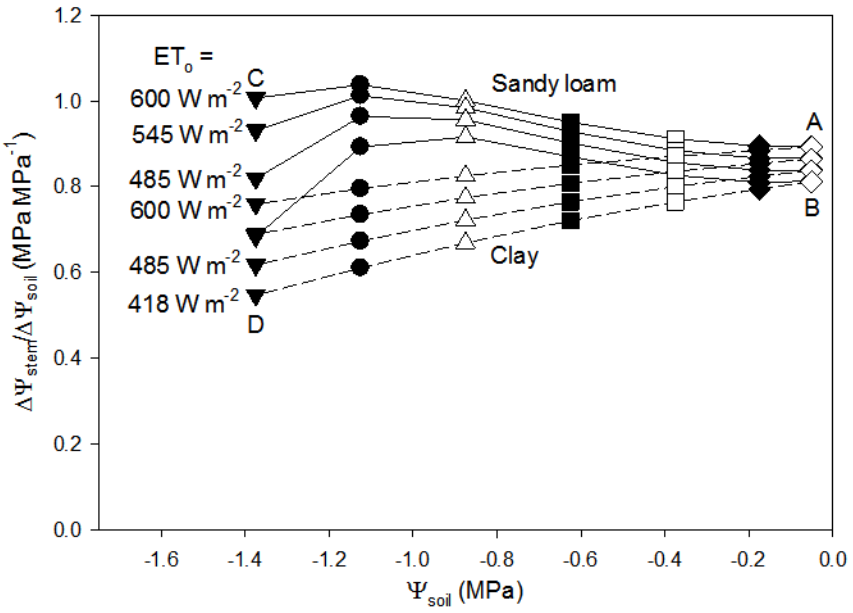

694

695 **Fig. 3** Change in sensitivity of Ψ_{stem} ($\Delta\Psi_{stem}/\Delta\Psi_{soil}$) in response to variation in Ψ_{soil} and ET_o for two soil

696 types. Data are the same as in Fig. 2.

697

698

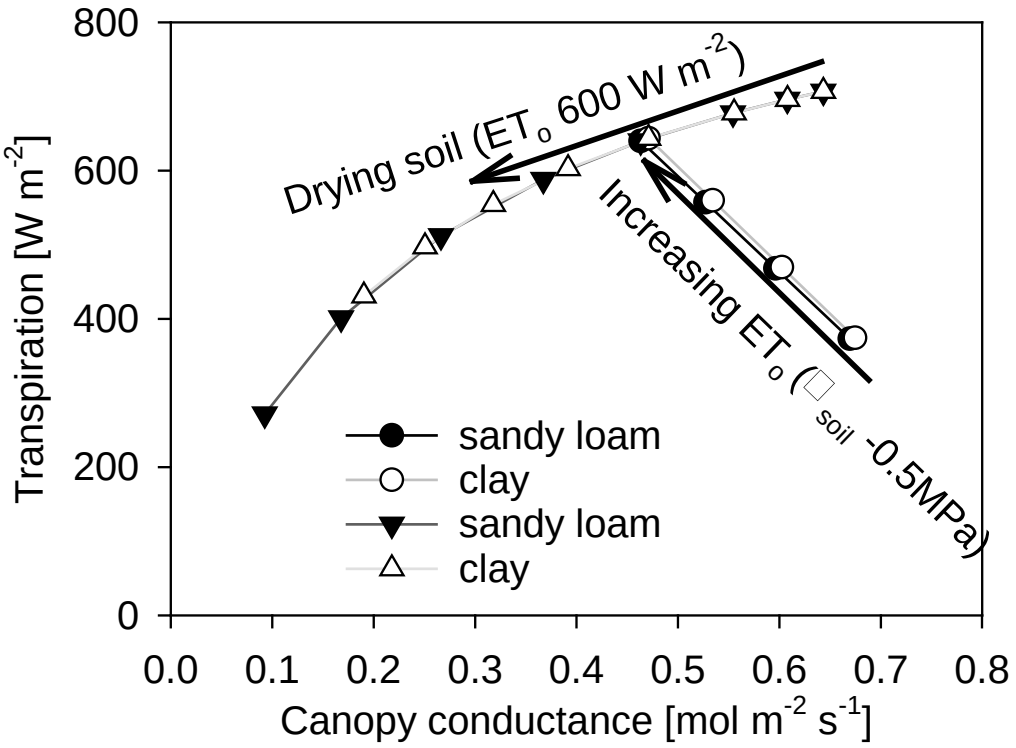

Fig. 4 A positive relationship between transpiration and stomatal or canopy conductance under varying Ψ_{soil} and a negative relationship under varying ET_o for a constant Ψ_{soil}. These data are the same as Fig. 2, restricted to the highest ET_o (and Ψ_{soil} varied) or a Ψ_{soil} of -0.5 MPa (and ET_o varied). The contrasting behavior of supply (circles) and demand (triangles) responses of transpiration to canopy conductance is evident at higher conductance.

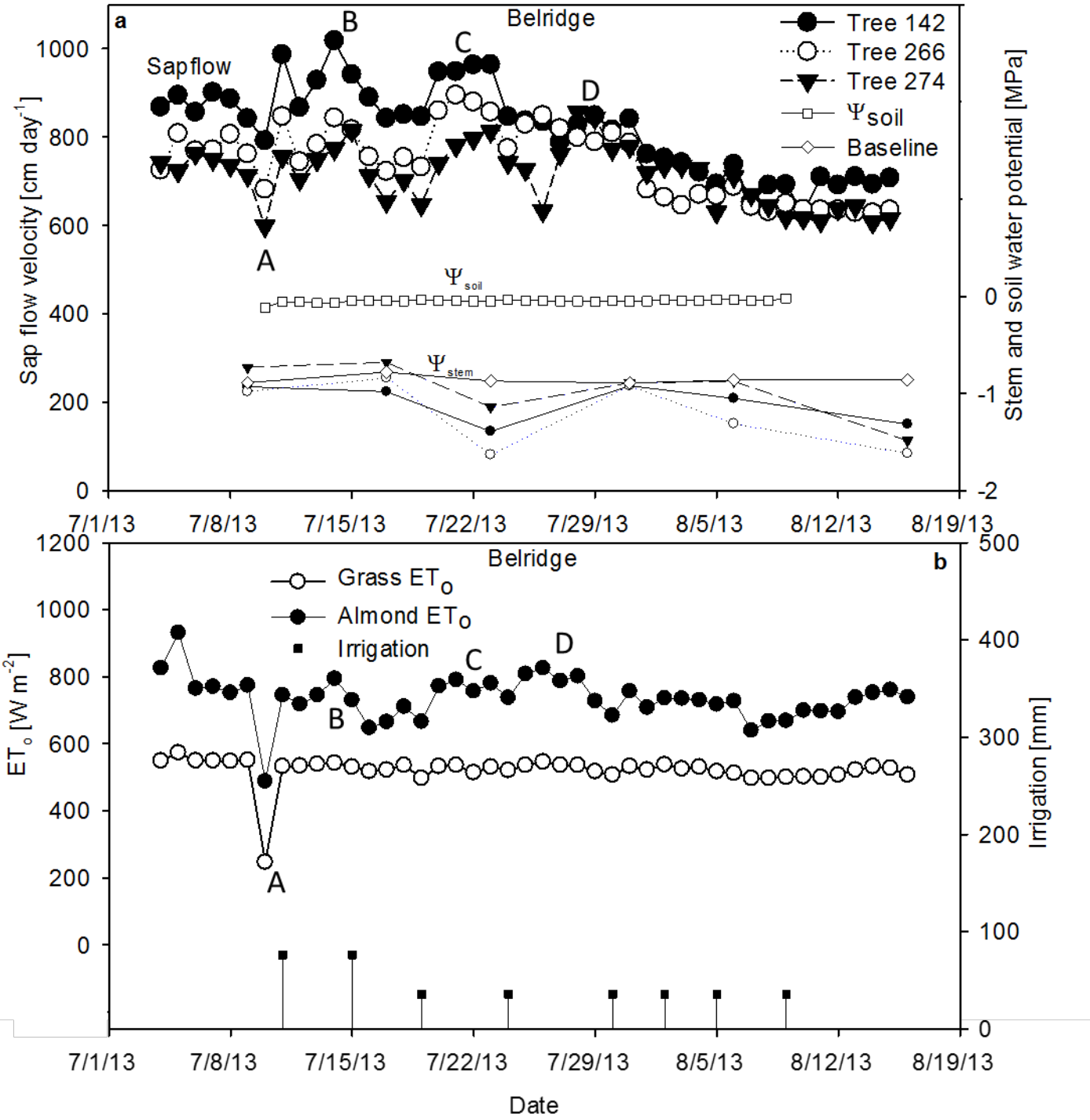

Fig. 5 Temporal pattern of daily cumulative sapflow velocity and stem water potential (Ψ_{stem}) of three trees at the Belridge site (a) and temporal pattern of grass reference evapotranspiration (ET_o, from FAO

711 56, Allen *et al.*, 1998) and almond reference evapotranspiration for midday conditions in Belridge (b).
712 Irrigation water applied and the baseline for stem water potential are also indicated. The soil water
713 potential (Ψ_{soil}) was estimated to illustrate when soil moisture was limiting.

714

715

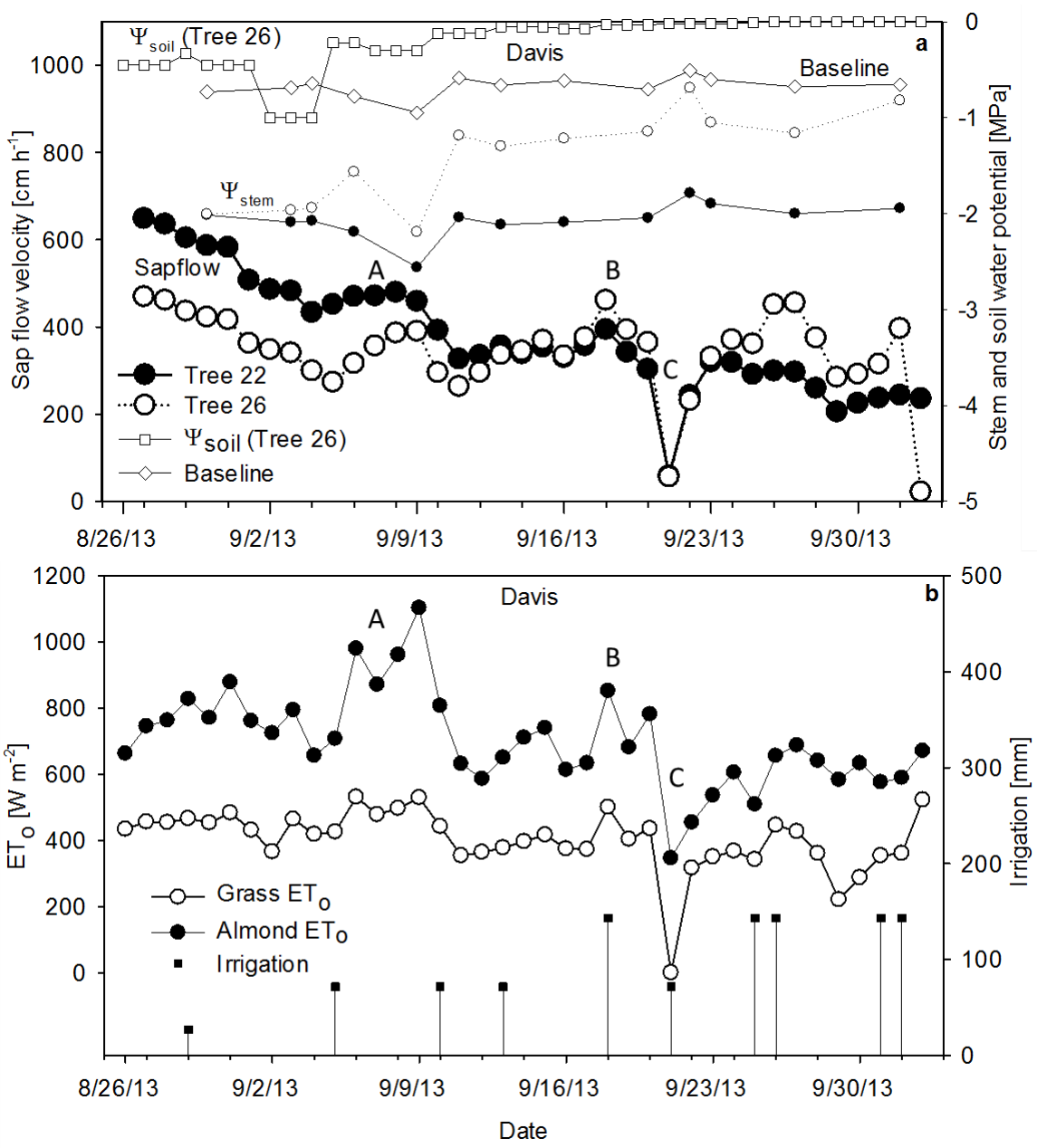

716

717 **Fig. 6** Temporal pattern of daily cumulative sapflow velocity and stem water potential (Ψ_{stem}) of three
718 trees at the Davis site (a) and temporal pattern of grass reference evapotranspiration (ET_o, from FAO 56,
719 Allen *et al.*, 1998) and almond reference evapotranspiration for midday conditions in Davis (b). Irrigation
720 water applied and the baseline for stem water potential are also indicated. The soil water potential (Ψ_{soil})
721 was estimated to illustrate when soil moisture was limiting.

722

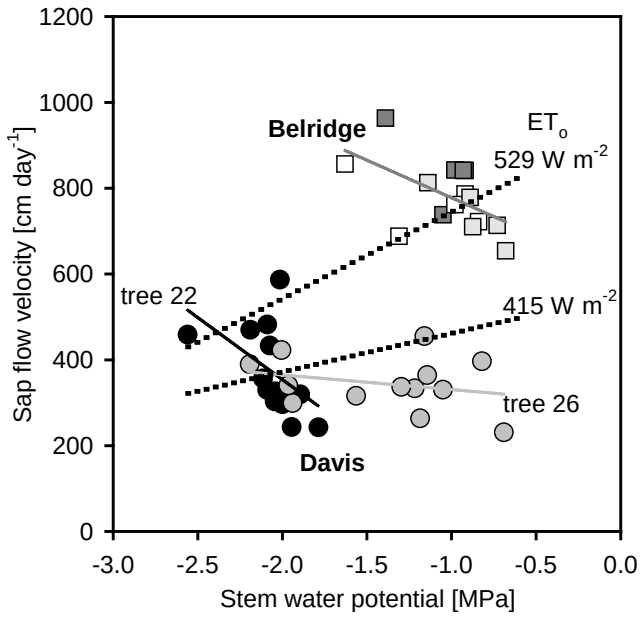

723

724 **Fig. 7** Sap flow velocity relationship with stem water potential for tree 26 in Davis (circles) undergoing
725 rehydration from water deficit, tree 22 in Davis under soil water deficit and varying ET_o (Fig. 6), and
726 three trees in Belridge (squares) with uniform irrigation and low variation in ET_o (Fig. 5). Dashed lines
727 are fitted relationships between sap flow and water potentials for two constant ET_o values (averages for
728 the two sites) derived from a multiple regression analysis: sap flow = $-879 - 317*\Psi_{stem} + 3.45*ET_o +$
729 $0.98*ET_o*\Psi_{stem}$ with $P < 0.001$, $P < 0.001$ and $P = 0.029$ for each factor, respectively.

730